A many-body potential for point defect clusters in Fe-C alloys

Timothy T. Lau[1], Clemens J. Först[1,2], Xi Lin[1,2], Julian D. Gale[3], Sidney Yip[1,2], Krystyn J. Van Vliet[1]
[1]*Departments of Materials Science and Engineering, and*
[2]*Nuclear Science and Engineering, Massachusetts Institute of Technology, Cambridge, Massachusetts 02139 USA; and*
[3]*Nanochemistry Research Institute, Curtin University of Technology, GPO Box U1987, Perth 6845, Western Australia*

Modeling the consequences of crystalline defects requires efficient interaction sampling. Empirical potentials can identify relevant pathways if the energetics and configurations of competing defects are captured. Here, we develop such a potential for an alloy of arbitrary point defect concentration, body-centered cubic α-Fe supersaturated in C. This potential successfully calculates energetically favored defects, and predicts formation energies and configurations of multicarbon-multivacancy clusters that were not attainable with existing potentials or identified previously via ab initio methods.

PACS numbers: 34.20.Cf, 61.72.y, 71.15.Pd, 62.20.x

Metastable crystalline alloys such as body-centered cubic (bcc) iron supersaturated with carbon exhibit impressive mechanical and physical properties that derive from a complex array of, and interaction among, crystalline defects. Although point defect clusters are critical to the microstructural stability and properties of such alloys, the material physics that governs interactions among interstitial atoms and vacancies remains poorly understood. Ab initio simulations (e.g., via density functional theory, or DFT [1]) provide accurate and physically realistic energetic calculations of static defect cluster configurations [2], but the associated computational expense requires efficient surveying and identification of possible / probable reaction mechanisms among defect clusters. Empirical potentials that can approximate the relevant energy landscape regimes present an attractive solution, and **facilitate efficient large-scale dynamic simulations**. Such **potentials** should not only provide reasonable estimates for crystalline properties, but should also provide at least a qualitatively accurate prediction of the locations and heights of the energy minima and saddle points in the energy landscape. Several hyperdynamic formalisms require relatively smooth potential energy surfaces, but many real material systems are actually characterized by multiple energy minima that describe both interesting and trivial dynamic events in the material response [3]. For metallic alloys supersaturated in a minor element, accounting for the existence and nature of these minima as defects form and interact is particularly important to understanding the mechanisms of deformation. Here, we develop such a many-body interaction potential that describes both the properties and carbon-vacancy point defect landscape (structure and formation energies) of bcc α-Fe alloyed with C.

Three existing empirical potentials [4–6] have been developed for ferromagnetic bcc α-iron containing carbon. **Rosato [4] and Johnson [5]** both accounted for Fe-Fe and Fe-C interactions; both neglect C-C interactions and are thus not intended to describe the behavior under high C concentrations. Ruda et al. [6] developed a many-body embedded atom method potential (EAM) that includes C-C interactions, affording predictions of behavior for increased C concentrations. While these potentials may approximate thermodynamic properties of C within the bcc Fe lattice, they are not intended to provide good descriptions of configuration-dependent processes such as point defect cluster reaction pathways. For example, the Ruda et al. potential predicts that C occupies tetrahedral sites of a bcc Fe lattice, whereas ab initio calculations [2, 7] favor the occupancy of octahedral sites. Further, of these potentials, the Rosato potential most faithfully reproduces the *energies* associated with incorporating single point defects (carbon interstitials, vacancies, or carbon-vacancy cluster) in bcc Fe [7]. However, we [2] and Domain et al. [7] have shown that the equilibrium *configuration* of a carbon-vacancy cluster (1C-1Va) should position the C atom approximately at the octahedral site of the bcc lattice, forming a $\langle 100 \rangle$ dumbbell with the vacancy without significantly distorting the lattice; the configuration favored by the Rosato potential severely distorts the local lattice (Fig. 1). Consideration of only the binding energy E_b for this defect cluster does not indicate this discrepancy, as the Rosato potential predicts $E_b = 0.52$ eV as compared to 0.44 eV obtained via DFT [7]. **Our DFT calculations show that, a**lthough Fig. 1 corresponds to a local energy minimum, the formation energy E_f of this defect cluster is 1.00 eV greater than that of the $\langle 100 \rangle$ 1C-1Va structure. The Rosato potential predicts then that the DFT-favored $\langle 100 \rangle$ 1C-Va configuration and dissociated C and Va are energetically comparable

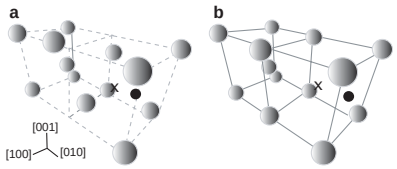

FIG. 1: (**a**) ⟨100⟩ C-Va cluster with distorted bcc structure favored by the Rosato potential. Dashed lines indicate bcc lattice for this defect cluster as predicted by our Fe-C potential and density functional theory (DFT) calculations (**b**). Fe atoms are shaded; relaxed position of the C atom (•) and the initial position of the Va (×) are shown.

states; DFT indicates the opposite [2, 7]. Thus, we aimed to develop a potential that could accurately render both energies and configurations of defects in an alloy with arbitrary point defect concentration.

As existing potentials were fitted to experimentally measured or computationally predicted (perfect) crystal properties, we hypothesized that a better description might be achieved by fitting the potential to the energies and also to the configurations of point defects and clusters thereof as predicted by DFT; this provides thermodynamic information as well as the dependence of energy on a large range of effective bond lengths. For this purpose, we adopted a many-body potential of the **Finnis-Sinclair (FS) formalism [8]**. Due to the need to provide descriptions of defect clusters including more than one C atom, we required a description of a C-C interaction. We have shown [2] that the dominant carbon-vacancy cluster over a range of temperatures, carbon concentrations (exceeding 1 wt.%C), and vacancy concentrations has at most three C atoms associated with each vacancy. Thus, we assumed carbon-rich environments would not form covalently-bonded nonplanar substructures requiring angular terms, and optimized the Fe-C interaction (up to the formation of the Fe_3C cementite phase) prior to developing the C-C interaction.

The energetic targets for defect clusters E_{dc} used to develop this potential (e.g., the energy of a 1C-Va cluster configuration) are simply the sum of the interaction potential energy minimum for lattice defects E_L (e.g., the energy of a single Va in bcc Fe in the relaxed state) and the DFT-obtained formation energy of the defect cluster $E_{f,dc}$ from bcc Fe with said lattice defect and from C atoms in vacuum. In order to obtain $E_{f,dc}$, we calculated the energy of the ground state spin-polarized C atom in vacuum with full occupancy in two of the p-orbital spin-up states. We approximated isolated atoms in a face-centered cubic unit cell of lattice constant a = 16 $\mathring{A}$, reasonably approximating the spherical symmetry of an isolated C atom, and reproduced the expected value of the cohesive energy of diamond as a check [10]. All DFT calculations were conducted as described in [2].

Ionic relaxation in DFT calculations was achieved using conjugate gradients (CG). To maximize the fitting database and achieve a greater degree of qualitative energy landscape feature correspondence between DFT and the potential, the geometries and respective energies of the relaxed defect clusters, unrelaxed defect clusters and select defect cluster configurations along the CG ionic minimization route were used [14]. Fitting was conducted with the GULP code [11] to optimize the weighted sum of squares of deviations in calculated and targeted energies, requiring physically reasonable behavior of the functions.

We adopted the many-body FS alloy format, where the total energy contribution of atom i is:

$$E_{\alpha,i} = -A_\alpha \sqrt{\sum_{j \neq i} \rho_{\beta\alpha}(r_{ij})} + \frac{1}{2} \sum_{j \neq i} \phi_{\beta\alpha}(r_{ij}) \tag{1}$$

Here, j refers to the nearest neighbors within a cutoff distance from atom i, α is the element type of atom i, β is the element type of atom j, A_α is a positive coefficient, $\rho_{\beta\alpha}(r_{ij})$ refers to the density contribution of j to atom i, and $\phi_{\beta\alpha}(r_{ij})$ refers to the pair interaction between atom i and its neighbors. Because this model adopts a density term which distinguishes the donor from the acceptor, addition of other alloying elements is enabled by this approach: pure element interactions represented by existing FS potentials could be readily incorporated without the need to develop a consistent set of A_α coefficients for each element, as required of EAM potentials.

We adopted Fe-Fe, Fe-C, and C-C interactions of the FS form used by **Rosato [4, 8]** for Fe-Fe:

$$\rho_{\beta\alpha}(r) \;=\; t_1(r - r_{c,\rho})^2 + t_2[(r - r_{c,\rho})^3],\; r \leq r_{c,\rho} \tag{2}$$

$$\phi_{\beta\alpha}(r) \;=\; (r - r_{c,\phi})^2(k_1 + k_2 r + k_3 r^2),\; r \le r_{c,\phi} \tag{3}$$

where these functions are zero for $r \ge r_c$. The constants r_c, t_i and k_i are provided in Tab. I. We confirmed the expected, exact agreement with experimentally determined lattice parameters and elastic constants (fitting targets in the original development of this Fe potential [8]), as well as the agreement of vacancy formation energies compared to experiments [9] and our DFT calculations [2]. From our fitting to an array of defect cluster targets (containing ≤1 C) partially listed in Tab. II, we obtained expressions for ρ_{Fe-C}, ρ_{C-Fe} and ϕ_{Fe-C} as shown in Tab. I. We then developed ρ_{C-C} and ϕ_{C-C} from the ensemble of nC and nC-nVa defect clusters indicated in Tab. II.

α	β	$r_{c,\rho}$	t_1	t_2	$r_{c,\phi}$	k_1	k_2	k_3
Fe	Fe	3.569745	1	0.504238	3.40	1.237115	-0.35921	-0.038560
Fe	C	2.545937	10.024001	1.638980				
					2.468801	**8.972488**	**-4.086410**	**1.483233**
C	Fe	2.545937	10.482408	3.782595				
C	C	2.892070	0	-7.329211	2.875598	22.061824	-17.468518	4.812639

TABLE I: Constants of the Fe-C potential developed in this work, assuming units of length in $\mathring{A}$ and units of energy in eV, where A_{Fe} = 1.8289905 eV and A_C = 2.9587870 eV. **Fe-Fe interaction parameter values and precision are those used by [4].**

Fitting target [eV]	This work	C-C Inter-[a] action	Ab initio	Rosato
C interstitial in perfect bcc lattice				
$E_{f,tet}$	- 6.38	No	- 6.25	- 5.03
$E_{f,oct}$	- 7.15	No	- 7.11	- 6.14
1C-1Va clusters[b]				
$E_{f,C}$	- 6.95	No	- 7.08	- 4.78
$E_{f,F}$	- 7.92	No	- 7.64	- 6.09
$E_{f,S}$	- 6.79	No	- 6.86	- 5.61
$E_{f,Fig.\ 1}$	- 7.15	No	- 6.64	- 6.64
2 C interstitials in perfect bcc lattice[c]				
$E_{f,\chi}$	- 13.45	Yes	- 13.38	N/A
$E_{f,\eta}$	- 12.33	Yes	- 12.27	N/A
2C-1Va clusters[d]				
$E_{f,AO}$	- 15.70	Yes	- 15.68	N/A
$E_{f,OO}$	- 15.25	Yes	- 15.27	N/A
$E_{f,\langle 110\rangle dumbbell}$	- 15.64	Yes	- 15.64	N/A
Fe_3C				
E_f	- 30.84	No	- 30.60	- 27.09

[a] Indicates whether C atoms are sufficiently distant ($\le r_{c,C}$) to require use of C-C interaction potential.

[b] C, F, and S denote, for a Va centered at (a/2, a/2, a/2), C positions at *approximately* bcc lattice corner (a/2, 0, 0), face-edge center (a/2, a/2, 0) and substitutional sites (a/2, a/2, a/2), respectively. For comparison, E_f corresponding to the configuration predicted by the Rosato potential in Fig. 1 is also given.

[c] Fe atoms at (0, 0, 0) and (a/2, a/2, a/2), where χ indicates C at *approximately* (a/2, a/2, 0) and (a/2, 0, a/2); η at (a/2, a/2, 0) and (a/2, 0, 0).

[d] AO denotes second C in adjacent octahedral position of 1C-1Va cluster; OO in opposite octahedral position.

TABLE II: Comparison of our Fe-C potential with experimental and ab initio data, including 2C-containing defects. Energies reported for Fe_3C and C interstitial(s) are relaxed states in reference to bcc Fe atoms and C atoms in vacuum; energies reported for nC-1Va clusters are relaxed states in reference to relaxed-bcc Fe atoms with Va already introduced in supercell and C atoms in vacuum. DFT and potential calculations, except for those of Fe_3C, used a 4x4x4 supercell under constant volume. Fe_3C results reported per unit cell cementite, with lattice constants a = 5.160 $\mathring{A}$, b = 6.658 $\mathring{A}$, c = 4.576 $\mathring{A}$ obtained from the potential fit and appropriately rescaled during fitting to account for small deviations from DFT lattice coordinates.

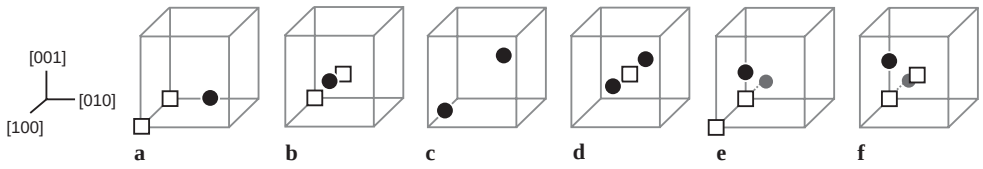

FIG. 2: Subset of the defect clusters in Tab. III that were correctly predicted, not fit, by our Fe-C potential. (a) 1C-2Va ⟨100⟩ dumbbell, with C at α (a/2, 0, 0), β (0, a/2, 0), or γ (-a/2, 0, 0); (b) 1C-2Va ⟨111⟩ dumbbell, with C at κ (a, a/2, a/2), or λ (a/2, a/2, 0); (c) 2C interstitials at μ (a/2, 0, 0) and (a/2, a, 0), or ν (a/2, 0, 0) and (0, a/2, a/2), or π (-a/2, 0, 0) and (a/2, 0, 0); (d) 2C-1Va ⟨100⟩ dumbbell; (e) 2C-2Va ⟨100⟩ dumbbell, with C pair located at *cp* (-a/4, 0, 0) and (0, 0, a/4), or *up* (0, -0.2a, -0.2a) and (0, 0.2a, 0.2a), or *sp* (-a/2, 0, 0) and (a/2, 0, 0); (f) 2C-2Va ⟨111⟩ dumbbell, with C pair located at *bp* (-a/2, 0, 0) and (0, -a/2, 0), or *vp* (-a/2, 0, 0) and (0, 0, a/2). C(•) and Va (□) approximate coordinates; Fe not shown.

We found that this interaction potential provides reasonable agreement with carbon-vacancy (nC-nVa) point defect cluster formation energies for defects that were determined by our ab initio calculations [2] and included explicitly in our ensemble of fitting targets (Tab. II), as well as those that were not explicitly targeted (Tab. III). **Note that DFT approximates the many-body electronic solution of Schrödinger via an assumed exchange-correlation energy functional [1]; these approximations can fail to reproduce experimentally measured surface energies of metals, resulting in monovacancy formation energy errors ≤0.15 eV for the cases of Cu and Al [12]. Here, our calculated monovacancy formation, migration, and self-diffusion (Q_{SD}) energies, as well as the volumetric lattice relaxation associated with a vacancy Ω_v/Ω_o, were in reasonable agreement with experimental results (Tab. IV).** Further, the presence of C interstitials in either octahedral or tetrahedral sites did not alter the elastic constants C_{ij} by ≥5 GPa, as expected from the insignificant effect of carbon concentration on elastic moduli for bcc Fe.

There are several features of this potential that demonstrate the utility of this approach in describing an energy landscape with competing energy minima. First, this potential correctly predicts the formation energy and configuration of a distinct phase, Fe_3C or cementite, which is stable even when relaxed under constant pressure (Tab. III). Second, this potential correctly predicts the stable configuration of the relaxed 1C-1Va defect cluster favored by the DFT calculations (Fig. 1b); the Rosato potential does not correctly predict this configuration (Fig. 1). Our molecular dynamics simulations performed using the LAMMPS code [13] at 1000 K followed by a quench to 0 K have not yet yielded a minimum for a 1C-Va configuration that is lower in energy. **Thus, beyond the designed match in energies of defect configurations between DFT and our Fe-C interaction potential, we found that DFT-predicted minima are also minima in our interaction potential when implemented in molecular statics or dynamics simulations.** Third, our interaction potential reasonably predicts the formation energies of many carbon-(di)vacancy clusters that were not included as fitting targets (Tab. III and Fig. 2). Fourth, the potential predicts previously unknown minima that we have subsequently verified using DFT. For instance, the ⟨100⟩ dumbbell 2C-1Va cluster favored by our potential (Tab. II) has not been reported by others [7] and has been identified as an energetically competitive minima by our own DFT calculations only after its discovery by our current potential. Although DFT does not favor this particular 2C-1Va cluster as the lowest in energy, the slight favoring of this configuration by our potential could be considered within reasonable fitting error. Finally, we have confirmed that unlikely defect configurations exhibit sufficiently greater (formation) energies as to be highly unfavored in the application of this potential to dynamic simulations. For example, DFT ranks the formation energy of the three energetically competitive 2C interstitial clusters that we considered in the same order as our potential indicates; our potential ensures by ≥ 1 eV that η and π clusters in Tabs. II and III, respectively, will be unfavored.

The potential developed herein can be applied to survey the defect energy landscape in a Fe-C alloy for arbitrary C concentrations including C-rich defect clusters. This enables, for example, identification of defect cluster mobility mechanisms to be explored further via computationally expensive band methods or rational function optimization of reaction pathways. Further, by targeting relevant point defect energies obtained by vacuum-corrected DFT simulations as outlined herein, this interaction model can be amended

Defect formation energy [eV]	This work	C-C Interaction[a]	Ab initio	Rosato
1C-2Va clusters (Fig. 2a)				
$E_{f,\alpha}$	- 7.67	No	- 7.99	- 4.89
$E_{f,\beta}$	- 7.98	No	- 7.69	- 6.08
$E_{f,\gamma}$	- 7.91	No	- 7.62	- 6.09
1C-2Va clusters (Fig. 2b)				
$E_{f,\kappa}$	- 7.93	No	- 7.74	- 6.09
$E_{f,\lambda}$	- 7.53	No	- 7.30	- 4.84
2 C interstitials in perfect bcc lattice (Fig. 2c)				
$E_{f,\mu}$	- 14.22	No	- 14.22	N/A
$E_{f,\nu}$	- 14.11	Yes	- 13.96	N/A
$E_{f,\pi}$	- 13.06	No	- 12.24	N/A
2C-1Va clusters (Fig. 2d)				
$E_{f,\langle 100\rangle dumbbell}$[b]	- 16.03	Yes	- 15.65	N/A
2C-2Va $\langle 100\rangle$ clusters (Fig. 2e)				
$E_{f,cp}$	- 15.74	Yes	- 15.75	N/A
$E_{f,up}$	- 15.51	Yes	- 15.88	N/A
$E_{f,sp}$	- 15.56	Yes	- 15.65	N/A
2C-2Va $\langle 111\rangle$ dumbbell clusters (Fig. 2f)				
$E_{f,bp}$	- 15.76	Yes	- 15.98	N/A
$E_{f,vp}$	- 15.72	Yes	- 15.51	N/A

[a]Indicates whether C atoms are sufficiently distant ($\leq r_{c,C}$) to require use of C-C interaction potential.
[b]This cluster resembles the 2C-1Va cluster in Table II (OO), but here the C-pair forms an approximate dumbbell with the Va.

TABLE III: Predictions of defect cluster formation energies from the Fe-C interaction potential developed in this work, as compared to those from our ab initio DFT calculations and the Rosato potential [4]. These defects were not fit targets in the development of our interaction potential. Energies are for relaxed states in reference to Fe atoms in a relaxed bcc structure with the appropriate (di)vacancy configuration already introduced in the supercell and C atoms in vacuum.

Quantity	Ab initio (DFT)	Experiments
$E_{f,Va}$ [eV]	2.02	1.59 - 2.04 [9]
$E_{m,Va}$ [eV]	0.96	0.16 - 1.28 [9]
Q_{SD} [eV]	2.80	2.36 - 3.01 [9]
Ω_v/Ω_o	0.93	0.95 [9]

TABLE IV: Comparison of calculated and experimentally reported vacancy formation and migration energies, self diffusion energy Q_{SD}, and lattice relaxation Ω_v/Ω_o associated with a vacancy in bcc α-Fe. $E_{m,Va}$ calculated from 4 x 4 x 4 supercell via nudged elastic band method, and Ω_v/Ω_o from comparison of fully relaxed supercells with/out a single vacancy.

readily **as ab initio approaches improve and as other alloying elements are added** in order to more faithfully recapitulate the energy landscape and defect dynamics of complex metastable alloys characterized by multiple energy minima and reaction pathways.

We gratefully acknowledge financial support from SKF Global, Inc., US National Defense Science and Engineering Graduate Fellowship program (TTL), and Western Australia Premiers Research Fellowship (JDG), as well as helpful conversations with J. Li, N. Marzari, and G. Ceder. We have benefited from computational resources funded by the US National Science Foundation (IMR-0414849).

[1] J.P. Perdew, K. Burke, and M. Ernzerhof, Phys. Rev. Lett. **77**, 3865 (1996).
[2] C.J. Först et al., Phys. Rev. Lett. **96**, 175501 (2006).
[3] B.P. Uberuaga et al., in *Handbook of Materials Modeling - Part A. Methods*, edited by S. Yip (Springer, Dortrecht, The Netherlands, 2005), 629.
[4] V. Rosato, Acta Metall. **37**, 2759 (1989).
[5] R.A. Johnson, G.J. Dienes, and A.C. Damask, Acta Metall. **12**, 1215 (1964).
[6] M. Ruda, D. Farkas, and J. Abriata, Scripta Mater. **46**, 349 (2002).
[7] C. Domain, C.S. Becquart and J. Foct, Phys. Rev. B **69**, 144112-1 (2004).
[8] M.W. Finnis and J.E. Sinclair, Phil. Mag. A **50**, 45 (1985).
[9] *Properties and Interaction of Atomic Defects in Metals and Alloys*, edited by H. Schultz, Landolt-Börnstein, New Series, Group III, Vol. 25 (Springer, Berlin, 1991), p. 128.
[10] X.J. Kong et al., Phys. Rev. B **42**, 9357 (1990).
[11] J.D. Gale and A.L. Rohl, Mol. Simul. **29**, 291 (2003).
[12] S. Kurth, J.P. Perdew and P. Blaha, Int. J. Quantum Chem. **75**, 889 (1999); K. Carling et al., Phys. Rev. Lett. **85**, 3862 (2000).
[13] S.J. Plimpton, J. Comp. Phys. **117**, 1 (1995).
[14] Many of the fit configurations have little significance beyond atomic coordinates; authors can be contacted for all configurations and corresponding fit results.